

Research on the Defect Detection System of Solar Cell Sheets based on the YOLOv9 Model

Zongyi Zhang*, Guoliang Wan

School of Mechanical Engineering, Tianjin University of Technology and Education, Tianjin 300222, China

*Corresponding Author

Abstract

A multi-station visual detection system is proposed to address the challenge of detecting various typical defects in solar cell sheets. To improve the detection accuracy of solar cell sheet defects, optimization of the YOLOv9 object detection model is explored. The introduction of the CBAM attention mechanism into the YOLOv9 model's backbone network enhances its ability to extract typical defects. The EIOU loss function replaces the original CIoU loss function, improving both the accuracy of the detection frame and the detection speed. Dynamic Snake Convolution (DSConv) is incorporated into the model to improve its recognition capability for small target defects. The effectiveness of the multi-station visual detection system and the superiority of the optimized model are validated through comprehensive stepwise and comparative experiments across different models.

Keywords

Solar Cell Sheets; Typical Defects; Multi-station Visual Detection; YOLOv9m; Model Optimization.

1. Introduction

Defects such as battery crack, cap crack, reverse cover, dislocation, and bubble are inevitable in the production process of solar cells, which seriously affect the photoelectric conversion efficiency of the cells and the overall service life of solar panels [1]. Therefore, users have put forward very high requirements for the qualification rate of solar cells produced by manufacturers. To ensure the qualification rate of the products leaving the factory, manufacturing enterprises need to hire a large number of quality inspectors to conduct comprehensive inspections on the cells after production. However, in the actual inspection process, the manual inspection method has problems such as high cost, low efficiency, heavy workload, easy fatigue, strong subjectivity, and inconsistent standards, which may lead to missed or false detections.

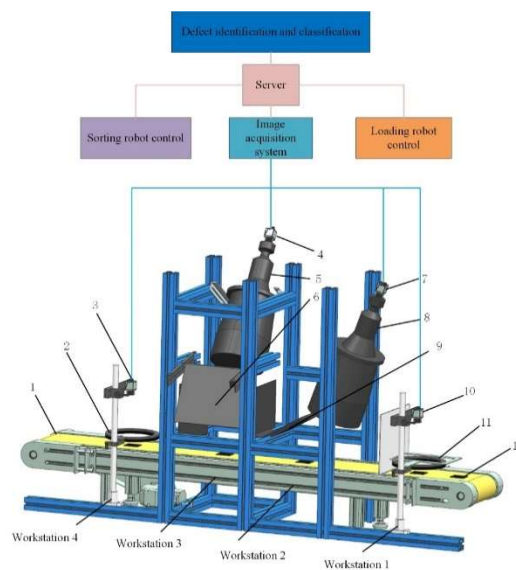
In recent years, with the development of deep learning and artificial intelligence, researchers have applied them to the surface defect detection of solar cells. Wang et al. constructed a deep learning network model based on the improved Faster R-CNN object detection algorithm, accurately classified defect types, and solved the problem of missed or false detections of solar cells caused by uneven light distribution [2]. Li et al. proposed an improved Faster R-CNN based on the Bidirectional Feature Pyramid Network (BiFPN), which combined the strong semantic information of high-level feature maps with the positional information of low-level feature maps to achieve high-quality extraction of multi-scale defect information [3]. Peng Xueling et al. based on the YOLOv5 algorithm, used Transformer as the backbone network and embedded the CBAM attention mechanism, which helped to improve the model's detection ability for small target defects [4]. Chen et al. designed a feature extraction network combining deformable

convolution and coordinate attention, which not only expanded the perception range of small target defects but also enhanced the recognition ability for small-sized defects. In addition, they improved the path aggregation network to reuse shallow features, thereby improving the detection accuracy [5]. Jiang Shangjun et al. proposed a solar cell defect detection method based on transfer learning and ResNet, which not only increased the training speed of the model but also improved the accuracy of solar cell defect detection [6]. Sezen et al. designed a visual defect detection method based on deep convolutional neural networks, calculated the surface quality loss of solar cells, and classified these losses through surface detection [7]. The above studies have improved the performance of solar cell defect detection models to a certain extent, but due to the complexity and diversity of solar cell defects, existing detection models still have problems of low detection accuracy and complex models.

To address the above issues, this paper proposes a multi-station visual inspection system and studies the optimization of the YOLOv9 object detection algorithm to achieve high-precision and high-efficiency detection of cell defects.

2. Design of Battery Defect Detection System

In this paper, according to the typical defect characteristics of solar cells, a set of multi-station visual inspection system is designed, and its system structure is shown in Figure 1. Here's how it works.



1, conveyor belt 2, ring light source 3, station 4 gray camera 4, station 3, gray camera 5, telecentric lens 6, panel light source 7, station 2 gray camera 8, telecentric lens 9, panel light source 10, station 1 gray camera 11, ring blue light source 12, battery

Figure 1. Solar cell defect detection system

Figure 1 In the detection system, the charging manipulator places the battery to be detected in the middle position of the conveyor belt in sequence according to the detection rhythm, and then inspects it successively. The sorting manipulator is mainly used to remove the tested battery from the conveyor belt, and classify and store the removed battery according to normal and different defect types.

Because there are many types of defects in solar cells, and there may be multiple defects in the same cell, the detection accuracy of different defects in solar cells can be significantly improved by using multi-station targeted detection. In Figure 1, the grayscale camera + blue light source

is used at station 1 to highlight the characteristics of battery crack defects. At station 2 and 3, a gray-scale camera plus a telecentric lens and a panel type high-light LED light source are used to highlight misalignment, cap reverse and bubble defects. At station 4, grayscale camera + ring LED light source is used to highlight the feature of cracked cover. The above four different stations of the camera with different light sources to achieve the acquisition of solar cell images, and present different defects, and achieved a better application effect.

3. YOLOv9 Model Analysis and Optimization

In order to improve the recognition accuracy of typical defects of solar cells, a variety of convolutional neural network models were studied, trained and tested in the early stage of this paper, and YOLOv9 model with good comprehensive detection performance was selected as the recognition model of battery defects. The basic structure and optimization measures of this model were analyzed below.

3.1. YOLOv9 Model Analysis

YOLOv9 adds Programmable Gradient Information(PGI) on the basis of previous YOLO series algorithms. PGI and Generalized Efficient Layer Aggregation Network (GELAN) [8]. PGI only uses the main branch in the model inference stage to ensure that the model does not generate redundant inference costs. The auxiliary reversible branch is introduced to generate reliable gradients and update parameters in real time, which reduces the loss of network information and improves the inference speed of the model. By eliminating the information bottleneck, GELAN can efficiently process the gradient information and update the weight of the model, so as to maintain the deep key information and finally complete the training and detection of the defect target. Considering the diversity and real-time requirements of solar cell detection tasks, in order to reduce the amount of subsequent manual review tasks, this study mainly improved the model from the perspective of model calculation accuracy and speed, taking YOLOv9 as the benchmark network:

- 1) The introduction of CBAM attention mechanism can effectively improve the detection algorithm's ability to identify small target defects.
- 2) replace the original model CIOU loss function to EIOU loss function, improve the quality of the battery defect target prediction box, and improve the regression accuracy of the prediction box.
- 3) Dynamic serpentine convolution is used to replace the standard convolution of the original model, which enhances the expressiveness and generalization ability of the model.

3.2. YOLOv9 Model Optimization Process

(1) Introduction of Convolutional Block Attention Module (CBAM) attention

The attention mechanism assigns different weights to different parts of the input data, allowing the model to dynamically choose which information to focus on based on the current task demands. CBAM attention mechanism combines spatial attention mechanism and channel attention mechanism, so that the model can better distinguish between target region and background region, effectively reduce background interference, improve detection accuracy, and reduce missed detection [9]. The CBAM attention mechanism structure is shown in Figure 2.

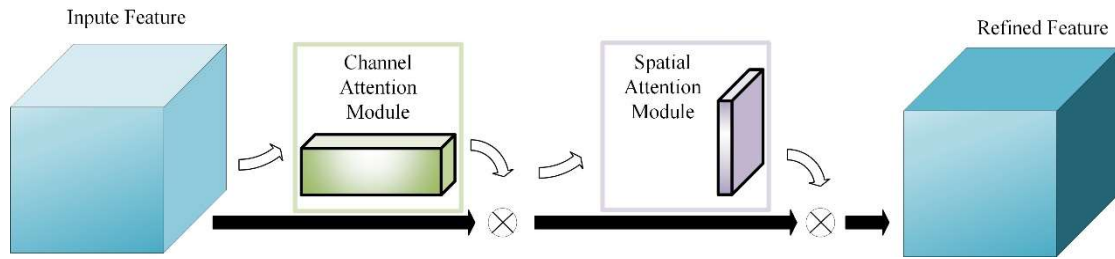


Figure 2. Structure of CBAM attention mechanism

In order to reduce the interference of complex environment and improve the model's ability to extract features, CBAM attention mechanism is introduced into the backbone network of YOLOv9 model to strengthen the network model's learning of defect features and improve the model's sensitivity to defects.

(2) Replace the loss function with EIOU

During object detection, IOU is often used to calculate the degree of similarity between the predicted results of the network and the real results. In view of the scattered location and large scale variation of defect features of solar cells, the CIOU loss function used in the original YOLOv9 is prone to problems such as poor boundary frame regression effect and inaccurate boundary frame positioning [10]. Compared with CIOU function, EIOU function can provide better optimization effect, improve model robustness and faster model training speed [11].

In this paper, the CIOU loss function of YOLOv9 is replaced by EIOU loss function to achieve a prediction frame with higher quality and improve the regression accuracy of the prediction frame.

(3) Introduce Dynamic Snake Convolution (DSCConv)

For the application of solar cell detection, the model is not only required to have a fast detection speed, but also to have a high detection accuracy. Compared with the standard convolution operation, dynamic snake convolution adopts the method of dynamically generated convolution kernel and flexible convolution path, which significantly improves the recognition ability of minor defects such as dislocation and cap crack [12]. The dynamic serpentine convolution structure is shown in Figure 3.

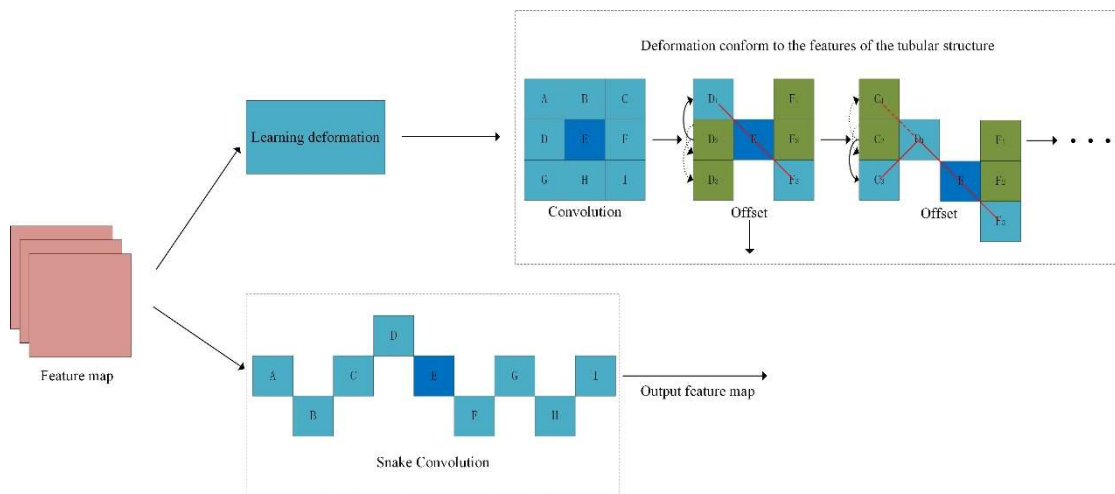


Figure 3. Dynamic serpentine convolution structure

In order to make the convolution kernel pay more attention to the processing of complex graphic features, deformation and offset variables are introduced to maintain the continuity of attention through iteration strategy. The specific change process is shown in Figure 4.

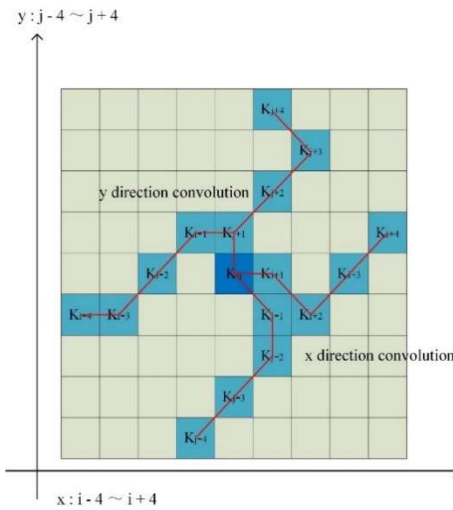


Figure 4. Dynamic serpentine receptive field variation map

Based on the small defects of dislocation and cap crack, the standard convolution of the original model is replaced by dynamic serpentine convolution, and the adaptive mechanism of dynamic serpentine convolution is used to make the convolution operation better deal with the feature information of dislocation and cap crack of solar cells, which enhances the expression and generalization ability of the model.

3.3. Improved Overall Network Structure of YOLOv9 Algorithm

The improved YOLOv9 algorithm introduces CBAM attention mechanism into the backbone network, which can effectively reduce background information interference and enhance the generalization ability of the model. The CIOU loss function is replaced by EIOU, which improves the accuracy of boundary frame positioning and solves the problem of slow convergence of boundary frame. The serpentine dynamic convolution is introduced to enhance the learning ability of the network for the misalignment and lacing features, and to improve the model's high sensitivity to small target features. The improved network model structure is shown in Figure 5.

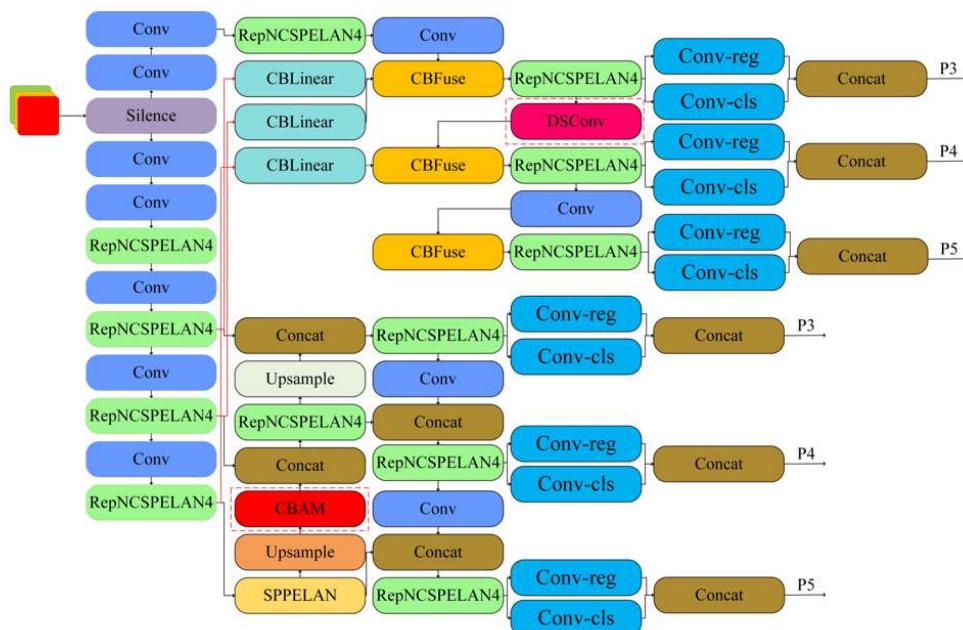


Figure 5. The improved YOLOv9 network structure

4. Experiment and Result Analysis

4.1. Experimental System Configuration Information and Parameter Settings

The operating system of the experimental hardware device is ubuntu 22.04, the processor CPU is 13th Gen Intel(R)Core(TM)i7-13700KF, and the GPU model is NVIDIA GeForce RTX 3090 with 24G video memory. The software environment is the programming language Python3.8, the framework Pytorch1.8.1, CUDA11.1.0 version and cuDNN11.1. In order to improve the convergence ability of the model, the size of the input image was set to 1080×1080, the parameter momentum was set to 0.937, the initial learning rate was set to 0.01, the batch_size was set to 4, and the iteration times epochs was set to 300 times.

4.2. Each Typical Defect Data Set Was Constructed

The research object of this paper is solar cells, and no open source data set is available at present. The equipment developed in the scheme in Figure 1 was used to re-detect the typical defective batteries manually detected by an enterprise, and the original data set was constructed. The number of typical defect images is shown in Table 1.

Table 1. The number of typical defect images

data set	dislocation	battery crack	bubble	cap crack	reverse cover	total
number of images (pieces)	1732	1525	1820	1875	1679	8631

4.3. Evaluation Index

In order to evaluate the model's detection effect on solar cell defects, the evaluation indicators used include: Precision (P), which refers to the probability of detecting positive samples in all the detected targets; R (Recall) refers to the probability of correct identification in all positive samples; Average Precision (AP) refers to the area under the accuracy and recall curves. It is used to evaluate the accuracy of the model during detection. Average Precision mAP (mean Average Precision) indicates the AP values of multiple types of targets. Detection speed FPS(Frames Per Second) : The number of images that can be detected per second.

4.4. Experimental Results and Analysis

In order to verify the superiority of the optimization method for the detection and detection of each typical defect target, step by step experiments were carried out on the test set data in the experiment, and the experimental results were shown in Table 2.

Table 2. Distributed experimental results

model	CBAM	EIOU	DSCConv	P	R	mAP	FPS(F/S)
YOLOv9	-	-	-	91.2	88.5	90.1	53.1
YOLOv9-1	√	-	-	91.0	90.3	91.8	57.2
YOLOv9-2	√	√	-	91.7	93.2	92.5	55.8
YOLOv9-3	√	√	√	93.3	93.5	93.6	56.8

As can be seen from Table 2, YOLOV9-1 introduced CBAM attention mechanism based on YOLOv9, mAP increased by 1.7 percentage points and FPS increased by 4.1F/S compared with the benchmark model. Based on YOLOv9-1, YOLOv9-2 uses EIOU loss function to replace the original CIOU loss function, and mAP further increases by 0.7 percentage points. YOLOv9-3 introduces DSCConv on the basis of YOLOv9-2, mAP increased by 1.1 percentage points, FPS increased by 1F/S. In addition, the comprehensively optimized YOLOv9-3 model also has

obvious advantages in the accuracy P, R and mAP parameters, which verifies the applicability of the optimized model to various defects of the battery.

Figure 6, 7, 8, 9 and 10 show the comparative detection results of various defects between the optimized model and the original model on the test set.

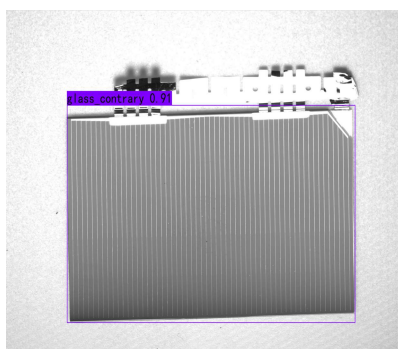


(a) Battery crack detection results before model optimization

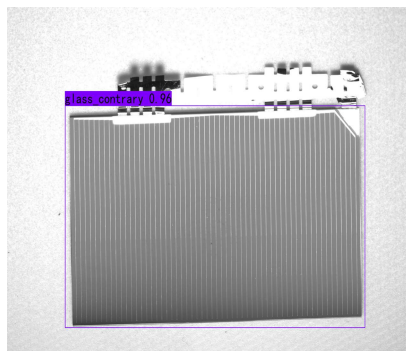


(b) Battery crack detection results after model optimization

Figure 6. Comparison of battery crack detection results before and after model optimization

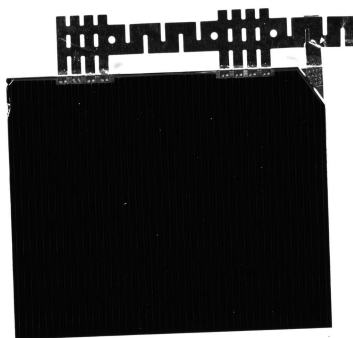


(a) Reverse cover detection results before model optimization

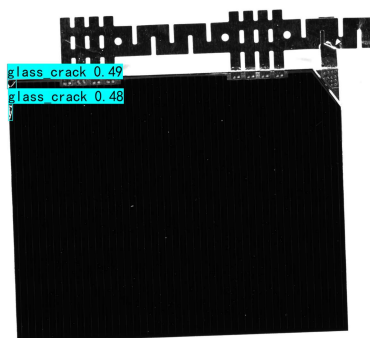


(b) Reverse cover detection results after model optimization

Figure 7. Comparison of reverse cover detection results before and after model optimization

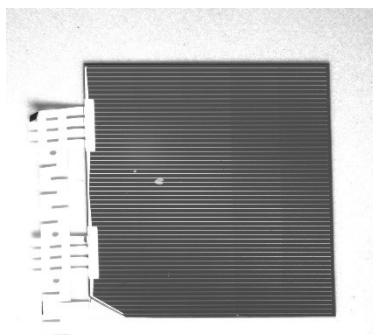


(a) Cap crack detection results before model optimization

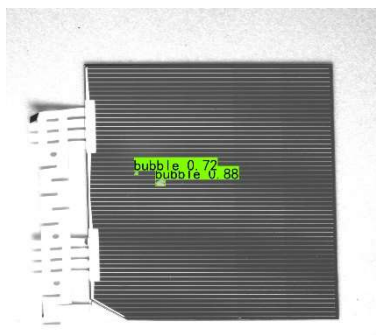


(b) Cap crack detection results after model optimization

Figure 8. Comparison of cap crack detection results before and after model optimization

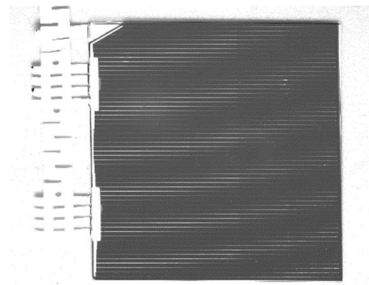


(a) Bubble detection results before model optimization

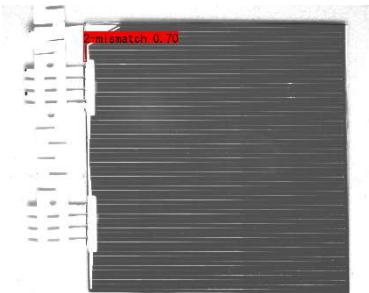


(b) Bubble detection results after model optimization

Figure 9. Comparison of bubble detection results before and after model optimization



(a) Dislocation detection results before model optimization



(b) Dislocation detection results after model optimization

Figure 10. Comparison of dislocation detection results before and after model optimization

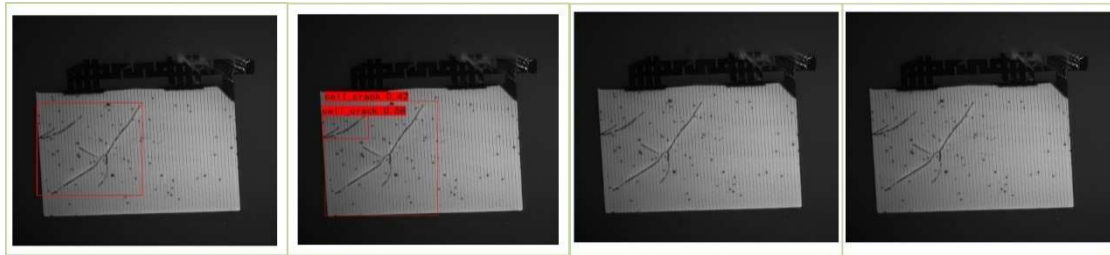
As can be seen from Figure 6 and 7, although both the original model and the optimized model can detect the battery crack and cover reverse defect of the battery, the confidence of the detection results of the optimized model has been greatly improved. It can be seen from Figure 8, 9, and 10 that the original model failed to detect the cap crack, bubble, and dislocation defects of the battery, while the optimized model successfully detected the defects of the battery with high confidence. The above step experiments further verify the applicability of the optimized model.

In order to further verify the applicability of the improved model to various defects of the battery, the optimized model was compared with SSD, YOLOv5, YOLOv7, YOLOv8 and other models in the same experimental environment. The experimental results are shown in Table 3.

Table 3. Comparison of detection performance among target detection models

model	P	R	mAP	FPS(F/S)
SSD	83.6	81.8	82.1	23.8
YOLOv5	77.0	81.1	79.2	71.4
YOLOv7	87.5	83.3	85.9	36.8
YOLOv8	93.6	85.5	88.1	44.6
YOLOv9	91.2	88.5	90.1	53.1
YOLOv9-3	93.3	93.5	93.6	56.8

As can be seen from Table 3, although P of the optimized model is slightly lower than that of the YOLOv8 model, other performance indicators of the optimized model are optimal. Figure 11-16 shows the comparison of the detection results of each model.

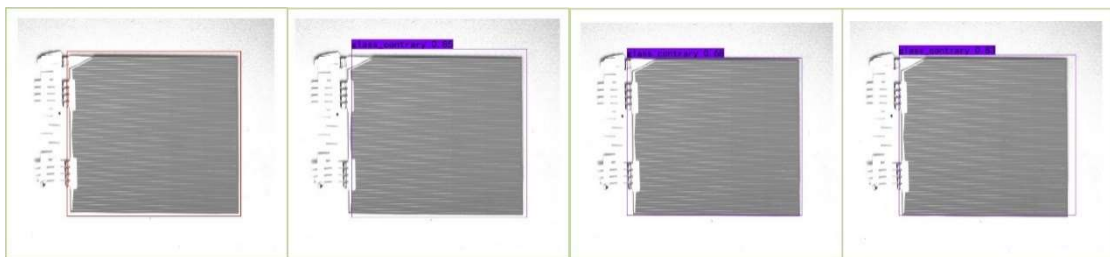


(a) Battery crack original (b) SSD detection result (c) YOLOv5 detection result (d) YOLOv7 detection result

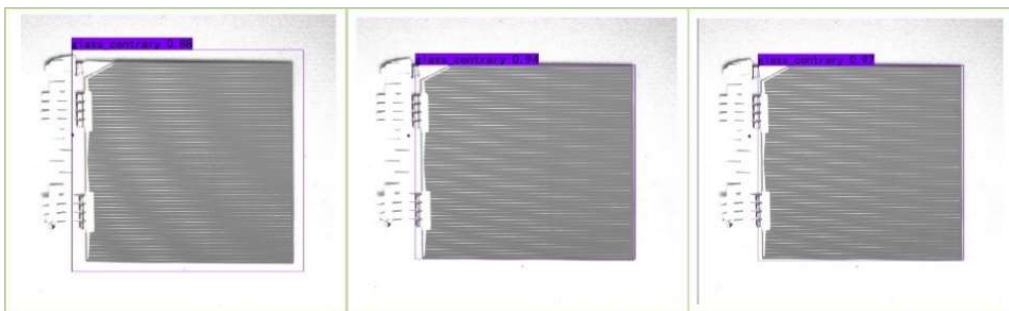


(a) YOLOv8 detection result (b) YOLOv9 detection result (c) Improved model results

Figure 11. The detection results of battery crack by each target detection model

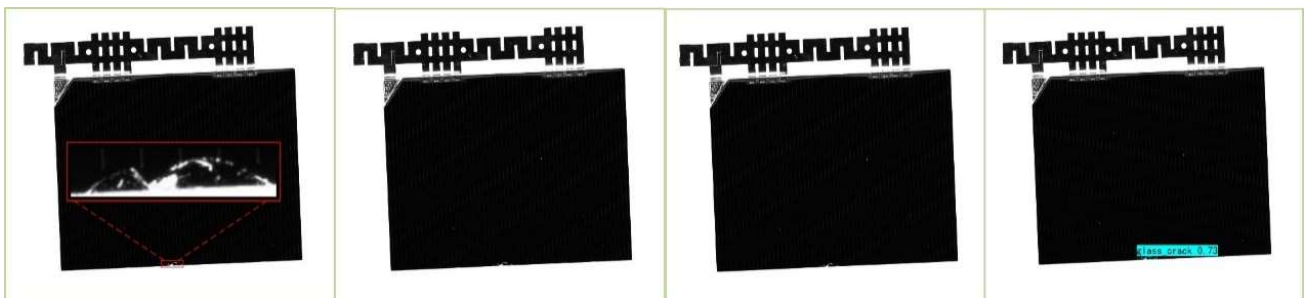


(a) Reverse cover original (b) SSD detection result (c) YOLOv5 detection result (d) YOLOv7 detection result



(e) YOLOv8 detection result (f) YOLOv9 detection result (g) Improved model results

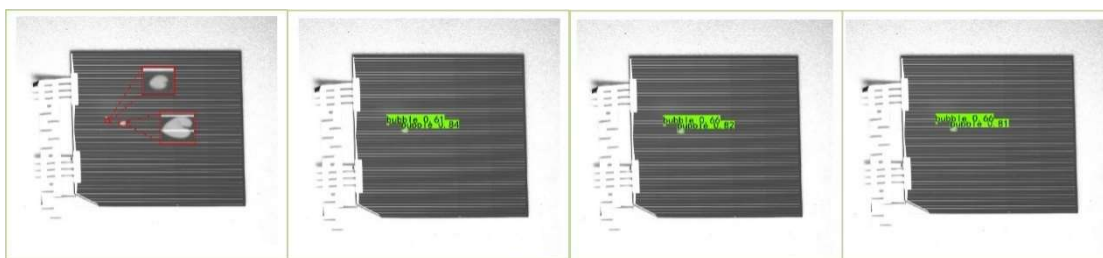
Figure 12. The detection results of reverse cover by each target detection model



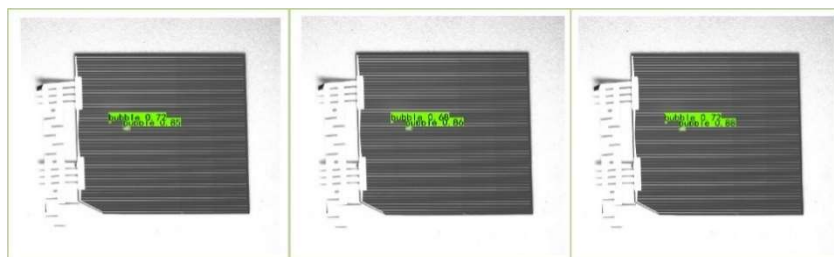
(a) Cap crack original (b) SSD detection result (c) YOLOv5 detection result (d) YOLOv7 detection result



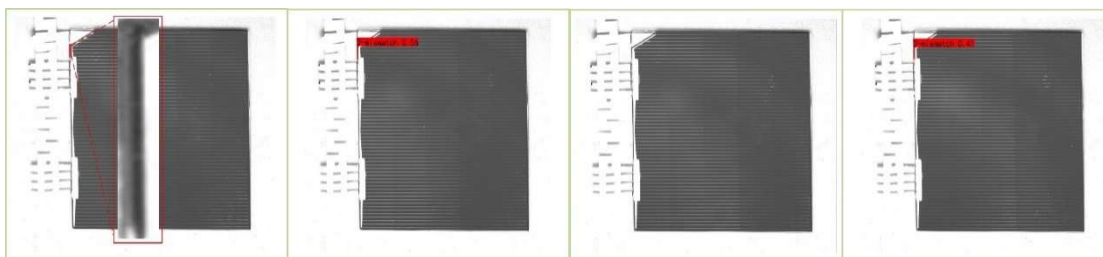
(e) YOLOv8 detection result (f) YOLOv9 detection result (g) Improved model results
Figure 13. The detection results of cap crack by each target detection model



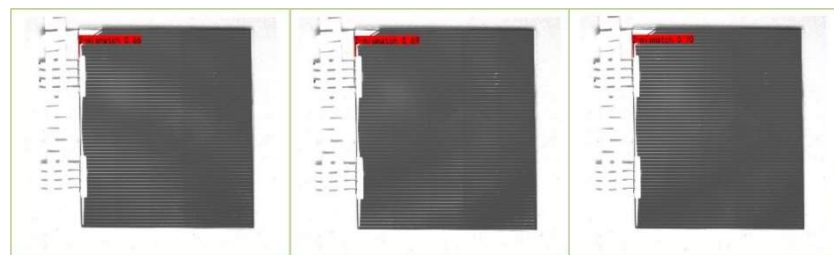
(a) Bubble original (b) SSD detection result (c) YOLOv5 detection result (d) YOLOv7 detection result



(e) YOLOv8 detection result (f) YOLOv9 detection result (g) Improved model results
Figure 14. The detection results of bubble by each target detection model



(a) Dislocation original (b) SSD detection result (c) YOLOv5 detection result (d) YOLOv7 detection result



(e) YOLOv8 detection result (f) YOLOv9 detection result (g) Improved model results
Figure 15. The detection results of dislocation crack by each target detection model

According to the test results in Figure 11-15, it can be seen that all models except the improved model have different cases of missing detection, and compared with other models, the improved model also has the highest confidence for various defects. The superiority of the improved model is further verified.

5. Conclusion

This paper carried out a comprehensive study on the optimization of the multi-station vision detection system for each typical defect of solar cells and the YOLOv9 target detection model. The main conclusions are as follows:

- (1) CBAM attention mechanism is introduced into the backbone network of YOLOv9 model to strengthen the network model's learning of various defect features. The CIOU loss function of the original model is replaced by EIOU, which improves the regression accuracy of the prediction box. DSConv was introduced to improve the recognition ability of small dislocation and cap crack defects. Step by step experiments show that the mAP value of the optimized model is increased by 3.5 percentage points, and the detection speed is increased by 3.7F/S.
- (2) The comparison experiment between the optimized model and other models in the same experimental environment shows that the comprehensive performance index of the optimized model has certain advantages. The confidence of all kinds of defect targets detected under the same conditions is the highest.
- (3) The proposed multi-station inspection visual inspection system can comprehensively reflect all kinds of defects of the battery, and are well reflected in the test results.

References

- [1] Li Zhenwei, Zhang Shihai, Qu Chongnian, et al. Defect detection for aerospace solar cells based on YOLOX-s algorithm. *Acta energiae solaris sinica*, Vol.45(2024) No.9, p. 276-284.
- [2] WANG J, ZHANG R, ZHENG X. Photovoltaic panel intelligent detection method based on improved faster-RCNN[C]//Proceedings of the IEEE 3rd International Conference on Electronic Technology, Communication and Information. Piscataway:IEEE Press,2023:1565-1569.
- [3] LI T, SUN Y. Defect detection of solar panels using improved faster R-CNN[C]//Proceedings of the International Conference on Image, Signal Processing, and Pattern Recognition. SPIE, Vol.127(2024) No.07, p. 605-610.
- [4] Peng Xueling, Lin Shanling, Lin Zhixian, et al. Defect detection algorithm of improved YOLOv5s solar cell. *Chinese Journal of Liquid Crystals and Displays*, Vol.39(2024) No.2, p. 237-247.
- [5] CHEN Yafang, LIAO Fei, HUANG Xinyu, et al. Solar cell defect detection using multi-scale YOLOv5. *Optics and Precision Engineering*, Vol.31(2023) No.12, p. 1804-1815.
- [6] JIANG Shang Jun, YI Hui, LI Hong Tao, et al. Defect detection method of solar cells based on transfer learning and ResNet. *Acta energiae solaris sinica*, Vol.44(2023) No.7, p. 116-121.
- [7] Sezen B, Cerasi C C. Solar cell busbars surface defect detection based on deep convolutional neural network[J]. *IEEE Latin America Transactions*, Vol.21(2023) No.2, p. 242-250.
- [8] Yang Shiman, Cao Zheng, Liu Nian Bo, Sun Yanli. Maritime Electro-Optical Image Object Matching Based on Improved YOLOv9. *Electronics*. Vol.13(2024) No.14, p. 2774-2774.
- [9] Woo S, Park J, Lee J Y, et al. Cbam: Convolutional block attention module[C]//Proceedings of the European conference on computer vision (ECCV). 2018: 3-19.
- [10] Du S, Zhang B, Zhang P, et al. An improved bounding box regression loss function based on CIOU loss for multi-scale object detection[C]//2021 IEEE 2nd International Conference on Pattern Recognition and Machine Learning (PRML). IEEE, 2021: 92-98.
- [11] Yang Z, Wang X, Li J. EIoU: an improved vehicle detection algorithm based on vehiclenet neural network[C]//Journal of physics: Conference series. IOP Publishing, Vol.1924(2021) No.1, p 012001-012006.

- [12] Nascimento M G, Fawcett R, Prisacariu V A. Dsconv: Efficient convolution operator[C]//Proceedings of the IEEE/CVF international conference on computer vision. 2019: 5148-5157.